INFLUENCE OF MICROSTRUCTURE ON FATIGUE FRACTURE CHARACTERISTICS OF Al_2O_3.

M. Kido*, G. Katayama*, Y. Tsuchibushi** and N. Inoda**

Fatigue fracture characteristics under static and cyclic loading were investigated for three kinds of Al_2O_3, with microstructures controlled by sintering additives (MgO, SiO_2+CaO) and particle size. The microstructures were fine equi-axed grains (Material M, MgO added), coarse columnar grains (Material SC, SiO_2+CaO added) and fine columnar grains (Material SC-f, SiO_2+CaO added). The crack propagation rates da/dN of Material SC was accelerated in water. The measurements of R-curve behaviour and COD under cyclic loading showed that the grain bridging effect of Material SC was reduced further than that of Material SC-f. In addition, surface analysis by EDX on fatigue fracture surfaces in Material SC showed that Si and Ca, the components of the sintering additives, were decreased markedly at SCG sites under cyclic loading in water.

INTRODUCTION

In recent years, the strength and toughening of ceramic materials have been actively investigated (1). To increase the reliability of structural materials, improved resistance to fatigue fracture is extremely important. However, the relation between microstructures and fatigue characteristics is largely unknown. It is important to clarify this relationship to obtain suggestions for practical future material development.

In this study, to improve fatigue fracture resistance in Al_2O_3, three kinds of Al_2O_3 ceramics, with microstructures controlled by sintering additives and particle size, were fabricated, and their fatigue behaviour was investigated. The influence of microstructure on fatigue fracture characteristics is discussed.

* Faculty of Engineering, Hiroshima Institute of Technology, Miyake, Saeki-ku, Hiroshima, 731-5127, Japan
**Graduate Student, Hiroshima Institute of Technology, Miyake, Saeki-ku, Hiroshima, 731-5127, Japan

EXPERIMENTAL PROCEDURE

Three kinds of Al_2O_3 ceramics were normally sintered at 1873K and prepared for the present work : Al_2O_3 powder of 99.9% purity (average grain size 1.8 μm) with 0.25wt% MgO (Material M); the above with 0.05mol% SiO_2+CaO having the same molar ratio (Material SC) as with the sintering additives; and Al_2O_3 powder of 99.99% purity (average grain size 0.15 μm) with 0.02mol% SiO_2+CaO having the same molar ratio (Material SC-f) as the sintering additive. The microstructures are shown in Fig.1. The mechanical properties are listed in Table 1. As shown in Fig.1, Material M has fine equi-axed grains with an average grain size of about 2 μm. Material SC has coarse columnar grains with a high aspect ratio, and Material SC-f has fine columnar grains.

TABLE 1 - Mechanical properties.

Material	Bending Strength σ_{b3} (MPa)	Hardness of Vickers	Fracture Toughness K_{IC}(MPa·m$^{1/2}$)	Weibull Modulus
M	320	1310	2.09	13.5
SC	320	1174	5.28	23.3
SC-f	346	1337	4.13	16.3

Test specimens 3 × 4 × 40(mm) and 5 × 10 × 50(mm) were used in this study, a pre-crack 1-2mm in length was made at the centre of it using a pre-crack device (BI method). The cyclic fatigue test was carried out by a fatigue testing apparatus using a piezoelectric bimorph as motive power, a symmetric four-point bending jig and a test tank made of Teflon. The test was carried out in air and in water, and test temperature was 293 ± 5K. Fracture surfaces were observed by scanning electron microscope (SEM), and the composition change at the fracture surface was analyzed by energy dispersive X-ray spectroscopy (EDX).

RESULTS AND DISCUSSION

Fatigue Crack Propagation Behaviour

Fig.2 and 3 show the relation between crack propagation rate, da/dN, and maximum stress intensity factor, K_{Imax}. The initial maximum stress intensity factors were set to 1.80MPa·m$^{1/2}$ for Material M, and 2.80MPa·m$^{1/2}$ for Material SC and Material SC-f, respectively. In Material M and Material SC-f , the crack did not propagate under static loading up to 10^5s, but did propagate under cyclic loading. This finding shows the influence of cyclic loading. No difference in crack propagation rate was observed between air and water. However in Material SC, the da/dN under cyclic loading was accelerated compared to static loading, and the acceleration was greater in water than in air. It is known that oxide ceramics are fatigued by stress corrosion cracking due to water (i.e., hydration reaction), as is glass. Thus, it is thought that this finding results from stress corrosion cracking due to water (i.e., hydration reaction) (2-3).

The comparison of these results shows that the K_{Imax} of Material SC and

Material SC-f were higher than that of Material M at the same da/dN. This difference was mainly due to the microstructures. As seen in Fig.1, Material SC and Material SC-f had columnar grains, which were highly resistant to fatigue crack propagation.

Generally, columnar grains more easily bridge the crack surface behind the crack tip. This becomes the stress shielding effect, which suppresses crack propagation. These relations are represented by the following equation (4) ;

$$K_{tip} = K_{apply} - K_S \quad \cdots\cdots (1)$$

where K_{tip} is the effective stress intensity factor at the crack tip, K_{apply} the applied stress intensity factor and Ks the K-value due to the stress shielding effect. Thus, K_{tip} increases and crack propagation is enhanced when the bridging effect corresponding to Ks decreases by fretting damage in the bridging region under cyclic loading.

Crack Opening Displacement

The crack opening displacement (COD) was measured under cyclic loading by mounting the strain gauge (the gauge length 5mm) to step over the crack, applying loads at which there was no crack propagation (about 35% K_{IC}) and running a fixed number of cycles for each material. Although the results are omitted, the curves show hysteresis. The existence of energy dissipation sites between the crack faces pushes the loading curve up and pulls the unloading curve down, causing the hysteresis loop. The area enclosed by the curve is the hysteresis energy , ΔE (5), due to grain bridging, which corresponds to Ks in Eq.(1) and makes a great contribution to toughness in ceramics. (Though the actual ΔE include many other factors, only the typical bridging effect was investigated in this study.) The results are listed in Table 2.

TABLE - 2 Comparison of the hysteresis energy ΔE of Material M, Material SC and Material SC-f.

Material	Number of Cycles N ($\times 10^5$)	Hysteresis Energy ΔE (J $\times 10^{-6}$)
M	0	1.92
	1	1.34
	3	0.78
	5	0.38
SC	0	10.85
	1	9.05
	3	6.75
	5	5.55
SC-f	0	9.12
	1	7.46
	3	6.91
	5	6.09

These results show that ΔE decreased with increases in the number of cycles in each material. This indicates that the bridging force controlled the crack opening, and closing was degraded due to fretting damage in the bridging region under cyclic loading. Thus, the stress shielding effect was decreased in steps under cyclic loading.

Although, the absolute values of ΔE can not be compared since the applied loads were different among these materials when measuring COD. The ΔE were made dimensionless by dividing the initial ΔE- value by ΔE_0, then compared as energy degradation rates. The results are shown in Fig.4. From this figure, $\Delta E/\Delta E_0$ decreases greatly during the first stage, then slowly after that in each material. In addition, degradation of Material M is greater than that of Material SC and Material SC-f. As seen in Fig.1, since the bridging effect in Material M is small, the influence of cyclic loading is also small. On the other hand, Material SC and Material SC-f suffered great damage under cyclic loading because their strength depends on the bridging effect.

For the reasons described above, it is believed that the acceleration of crack propagation rates under cyclic loading was caused mainly by the degradation of the bridging effect, which was most pronounced in Material SC.

A Consideration of Fatigue Crack Propagation Mechanism

It has already been mentioned that the da/dN under cyclic loading in Material SC was accelerated in water. The composition change at fatigue fracture surfaces in Material SC was subsequently analyzed by EDX. The results are listed in Table 3. A comparison of compositions in SCG (Slow crack growth) regions with those of unstable fracture regions shows that the presence of Si and Ca was markedly decreased at SCG sites in fatigue fracture surfaces. This indicates that these compositions dissolved as the fatigue crack propagated. In addition, the decrease in Si and Ca at SCG sites in cyclic fatigue fracture surfaces in water was greater than that of other fatigue fracture surfaces. It is thought that the hydration reaction was promoted such that fretting damage occurred in bridging regions under cyclic loading in water.

TABLE 3 - EDX analysis of fracture surfaces of Material SC.

	Static Fatigue in water		Cyclic Fatigue in air		Cyclic Fatigue in water	
Composition / wt%	SCG	U.F.*	SCG	U.F.*	SCG	U.F.*
Al	81.47	80.78	83.89	80.65	81.47	80.92
Si	6.46	6.66	6.88	6.97	6.05	7.21
Ca	12.10	12.40	11.85	12.25	10.08	12.37

* : Unstable Fracture

It is known that SiO_2 bonds break due to the hydration reaction (2-3). In this study, since the grain boundary of Material SC was glass phase consisting of SiO_2, etc., which were the additives, it is thought that the glass phase was more easily dissolved by the hydration reaction caused by water molecules. Moreover, the hydration reaction was accelerated by mechanochemical reactions at the crack tip, forming a high stress field where the crack propagated, dissolving the compositions of the grain boundary phase. This is called static fatigue. On the other hand, since the stress at the crack tip increases with the reduced bridging effect caused by wear in the bridging region and the dissolution of the grain boundary phase under cyclic loading, crack propagation was accelerated due to enhanced static fatigue. Consequently, it is thought that an increases in the stress at the crack tip due to the reduced bridging effect under cyclic loading promotes static fatigue. These results indicate that, the influence of environment being equal, less grain boundary phase is better. In addition, though

columnar grains are required for toughness, smaller grains are better since less fretting damage occurs in bridging parts under cyclic loading. In Material SC-f, the degradation of bridging effect was slight, and the hydration reaction was restrained because its grain boundary phase was less than Material SC. Thus, the degradation of fatigue strength in Material SC-f was less than that in Material SC.

From the above findings, the improvement of fatigue fracture characteristics of Al_2O_3 will require control of microstructure, including both grain morphology and grain boundary phase.

CONCLUSION

Three kinds of Al_2O_3 ceramics, with microstructures controlled by sintering additives and particle size, were fabricated, and their fatigue behaviour investigated. The results obtained are as follows.

(1) The crack propagation rate da/dN of Material SC was accelerated in water. This derived from Material SC containing more grain boundary glass phase than the other materials, which facilitated stress corrosion cracking by water. Consequently, crack propagation in Material SC was accelerated under cyclic loading in water.

(2) A comparison of energy degradation rates found that Material SC and Material SC-f had higher stress shielding effects due to grain bridging in the crack wake region, resulting from their microstructures.

(3) The results of analysis of fatigue fracture surfaces in Material SC under static and cyclic loading by EDX showed that Si and Ca were decreased at SCG sites, the decrease being greatest under cyclic loading in water. Consequently, it is believed that the hydration reaction at the grain boundary glass phase was more active under cyclic loading than under static loading. Thus, though there are some differences between materials, it is thought that the fatigue fracture characteristics in each material can be explained by a model of stress corrosion cracking at the grain boundary phase.

REFERENCES

(1) S.Horibe and R.Hirahara, Acta Metall. Mater., Vol.39, No.6, 1991, pp.1309-1317.

(2) T.Okabe, G.Katayama, M.Kido and N.Udaka, Mater. Sci. Res. Int., Vol.2, 1996, pp187-192.

(3) S.M.Wiederhorn, E.R.Fuller Jr and R.Thomson, Metal Science, Vol.14, No.Aug-Sep, 1980, pp.450-458.

(4) A.Ueno, H.Kishimoto, S.Ookawara, T.Kondo and A.Yamamoto, J. Soc. Mater. Sci., Japan, Vol.43, No.485, 1994, pp.183-189.

(5) G.Vekinis, M.F.Ashby and P.W.R.Beaumont, Acta Metall. Mater., Vol.38, No.6, 1990, pp.1151-1162.

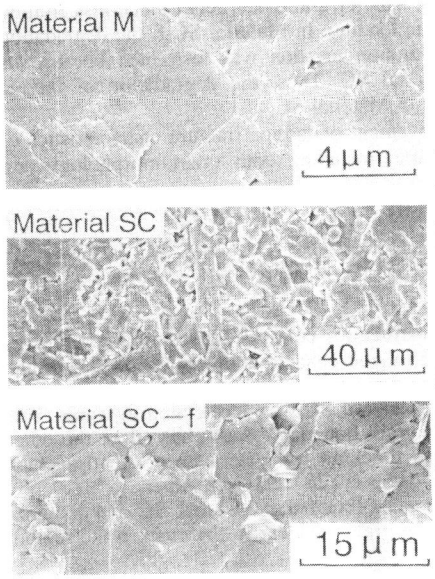

Figure 1 SEM observation of etched surfaces.

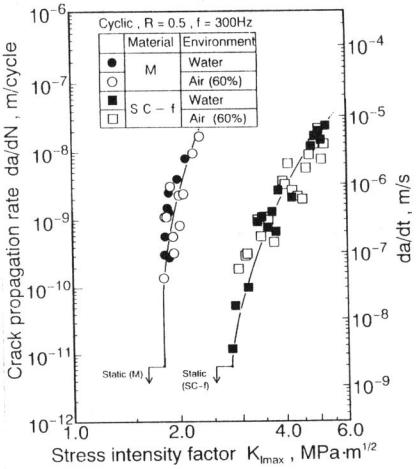

Figure 2 Relation between da/dN and KImax in Material M and Material SC-f.

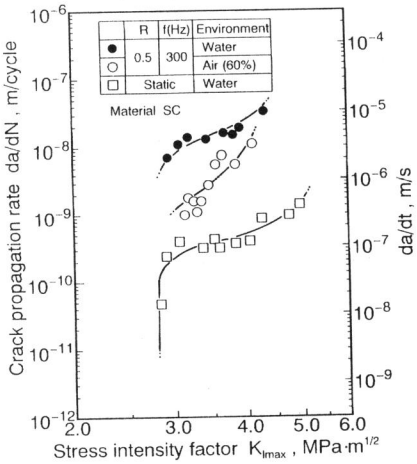

Figure 3 Relation between da/dN and KImax in Material SC.

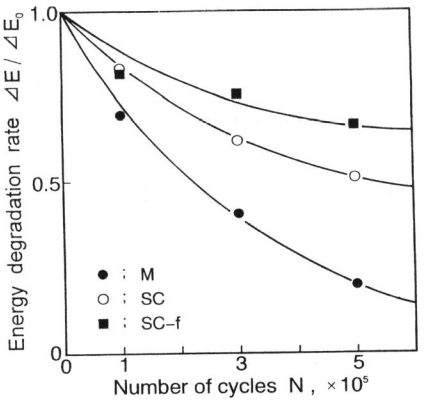

Figure 4 Relation between ⊿E/⊿E0 and N.